Scanning electrochemical microscopy for the investigation of localized degradation processes in coated metals: Effect of oxygen

Sergio González, Juan J. Santana[+], Yaiza González-García and Ricardo M. Souto

Department of Physical Chemistry, University of La Laguna, E-38207 La Laguna, Tenerife, Canary Islands, Spain

Abstract

The effect of oxygen content on the corrosion reactions inside a holiday in a polymer-coated metal substrate was studied by SECM without adding a redox mediator. The system was mild steel coated by polyurethane in KCl. By selecting different values for the potential applied to the ultramicroelectrode tip, local concentrations of species involved in the degradation process are monitored, namely Fe(II) ions, hydrogen peroxide and oxygen. The results show a variation in both the shape and the magnitude of the scan lines measured over the holiday. A critical oxygen concentration was found below which the corrosion reaction is not observed.

Keywords: A. Organic coatings; A. Polyurethane; A. Mild steel; B. Scanning electrochemical microscopy; C. Iron dissolution; C. Oxygen reduction.

[+] On leave from the Department of Process Engineering, University of Las Palmas de Gran Canaria, Campus Universitario de Tafira, E-35017 Las Palmas de Gran Canaria, Canary Islands, Spain.

1. Introduction

With the advent of scanning electrochemical microscopy (SECM), *in situ* studies of localized corrosion at polymer-coated metals with high spatial and chemical resolution have become possible [1-4]. The uptake of reactants from the electrolyte phase through the polymeric matrix to metal/polymer interface have been imaged by negative-feedback SECM [5-8]. In this way, the earlier stages of blistering processes have been imaged, and the growth kinetics of single blister could be followed [9]. Operation of the SECM in the feedback mode requires the diffusion towards the tip of a redox species, called the redox mediator, to occur in the electrolytic phase, and this substance to be either oxidized or reduced at the tip which acts as a ultramicroelectrode (UME). The faradaic current involved in this redox process is the physicochemical property considered for the near field effect. That is, when the tip is located in close proximity to the substrate under investigation, the current measured is greatly affected by the tip-substrate distance. Depending on whether the substrate is a conductive or an insulating surface, the feedback effect detected at the UME will be either positive or negative, respectively [10]. The main disadvantage of this operation mode originates for the investigation of non-defective coatings is that the redox mediator substance must be added to the electrolytic phase, and the possible permeation of this species through the polymeric matrix, both affecting the chemical and the electrical condition of the coated sample, cannot be discarded at priori. The use of the oxygen naturally dissolved in the electrolyte as redox mediator has been proposed [11], though the irreversibility of the reduction reaction at the tip and the concentration gradient in the electrolyte with the distance to the surface of the liquid phase, greatly limits the sensitivity of the technique. This procedure was successfully employed to confirm the specific effect of chloride ions towards early blistering previously reported when the surface of the coated metal was imaged using ferrocene-methanol as redox mediator [12].

Additionally, the ability of scanning electrochemical microscopy to resolve the spatial distribution of electroactive species allowed the *in situ* monitoring of electrochemical reactions occurring inside defects in the polymer layer to be carried out and show the relationship between electrolyte composition and the extent of the corrosion reaction [13-16]. When the SECM operates in the sample generation – tip collection mode, the faradaic current measured at the UME results from the redox conversion of a species produced during the corrosion reaction at the substrate. The adequate selection of the potential applied at the tip allows the discrimination of the locations on the sample at which the reaction is actually occurring [17], as well as to monitor the possible migration of reaction sites on the surface as result of activation/deactivation processes [18]. In this way, the corrosion reactions occurring at the metal/electrolyte interface in defects through a polymeric coating, the time evolution of oxidized metal species originating from the anodic reaction and the consumption of the species participating in the cathodic process could be followed [13,14]. In a previous paper, carbon steel samples coated with polyurethane in which a holiday was produced prior to immersion in different aqueous electrolytes were investigated with this technique. The release of Fe(II) ionic species into the solution phase from local anodic sites, as well as the consumption of dissolved oxygen at the corresponding cathodic locations was successfully monitored [13].

The object of this work was to investigate the effect of oxygen on the corrosion reaction occurring in a holiday produced through a polyurethane-coated carbon steel sample. The oxygen content in the

electrolytic phase was carefully modified in the electrochemical cell, and the SECM technique was employed to detect the local concentration of electroactive species Fe^{2+}, H_2O_2 and O_2, which are involved in the corrosion reaction.

2. Experimental

2.1. Materials

Mild steel plates of dimensions 2 cm x 2 cm were employed in this work. After cleaning and degreasing with acetone, a polyurethane coating (*Sigma Semigloss* from Sigma Coatings, Amsterdam, The Netherlands) was applied to the substrate using a draw-down bar following the procedure described elsewhere [19]. The coupons were allowed to cure for a week at room temperature and humidity prior to testing. The dry film thickness of the resulting coating was around 90 µm as measured using a Mega-Check FN coating thickness-meter (List-Magnetik GmbH, Germany). Artificial circular defects in the organic coating were produced by using a driller to produce a holiday of 170 µm diameter. The samples were then exposed to deaerated aqueous solutions at room temperature (20 ºC), and examined using SECM at regular intervals. The test electrolyte was 0.1 M KCl prepared using analytical grade chemicals.

2.2. Instrumentation

The SECM instrument used in these experiments was a CH900 scanning electrochemical microscope (CH Instruments, Austin, TX, USA), controlled with a personal computer. The system was placed inside an active isolation workstation, which effectively isolated the system from electrical and acoustic noise as well as from mechanical vibrations. Control of the microelectrode was performed using a step motor driven *x-, y-, z*-stage capable of reproducible three dimensional motions. The system was operated in a three-electrode configuration since the coated sample was left unbiased during experiments at its corresponding open-circuit potential.

The tip electrode was a 10 µm dia. platinum microelectrode as the probe, an Ag/AgCl/KCl(sat.) reference electrode, and a Pt wire counter electrode, all set up in a cell made of polytetrafluoroethene. Specimens were mounted horizontally facing upwards. In all experiments the coated sample was used unpolarized at its open-circuit corrosion potential. The micromanipulator stand of the SECM instrument was used to hold the microelectrode in place. Scans were conducted both vertically (approach curves) and parallel to the sample surface. In the latter case, the measurements were performed with the microelectrode at a constant height of 10 µm over the specimen surface.

2.3. Experimental procedure

The approach of the tip to the substrate was performed by monitoring the reduction of oxygen at the microelectrode in the naturally-aerated 0.1 M KCl test solution. To enable the reduction of oxygen, the tip was kept at a constant potential of -0.70 V vs. Ag/AgCl/KCl(sat.) [7]. The operating distance of the microelectrode tip over the coated surface was established by measuring the corresponding approach curves at a location sufficiently far from the holiday. After the experimental curves were fitted to the theoretical model for negative-feedback behaviour, and the exact tip-distance could thus be determined, the tip was retracted from the surface to a height of 10 µm which was set as the tip-substrate distance for the experiments measured parallel to the surface.

The tip potential was set at different values to investigate the local concentrations of the various species involved in the corrosion process. The selected values were +0.60 V vs. Ag/AgCl/KCl(sat.) to monitor the oxidation of Fe(II), +0.25 V vs. Ag/AgCl/KCl(sat.) for the oxidation of hydrogen peroxide generated in the cathodic reaction, and at -0.70 V vs. Ag/AgCl/KCl(sat.) for the reduction of soluble oxygen. Line scans were acquired by moving the microelectrode in a raster-type motion, and they were measured in the scan direction using a step/acquire scheme where the step size was 10 µm. The scan rate was 50 µm s^{-1}.

The oxygen contents in the electrolyte were modified by purging the electrolyte with nitrogen for various controlled periods of time, and the subsequent effect of this treatment on the corrosive process was studied by recording scan lines at constant height passing over the holiday. Alternately, oxygen was removed by heating the solution to 60 ºC, and subsequently allowing the solution to cool down back to 20 ºC under nitrogen atmosphere.

3. Results and discussion

3.1. Monitoring of iron soluble species in the proximity of the holiday during immersion in 0.1 M KCl when oxygen is removed from the electrolyte

By setting the tip potential to +0.60 V vs. Ag/AgCl/KCl(sat.), the oxidation of the Fe(II) species dissolved in the electrolyte can be detected through their oxidation to Fe^{3+} at the UME.

$$Fe^{2+} \rightarrow Fe^{3+} + 1e^- \qquad E^0 = +0.548 \text{ V vs. Ag/AgCl/KCl(sat.)} \qquad (1)$$

Since no Fe(II) species were originally present in the electrolytic phase, they can only originate from corrosion processes at the metal directly exposed to the aqueous environment inside the holiday. In this way, soluble Fe^{2+} ions would diffuse away from the volume inside the holiday and will be eventually detected at the tip through their oxidation. Therefore, the measurement of a faradaic current different from zero at the tip would probe the corrosion of the metal inside the defect. It must be noticed that the electrons released by iron will be consumed by soluble oxygen in the cathodic half-reaction.

Figure 1 depicts consecutive scan lines recorded over the holiday after the electrolyte was purged with nitrogen gas for various times as indicated in the plot. The gas flow was forced to pass through the

electrolyte in the period compressed between the measurements, whereas it was maintained passing over the cell during the actual SECM measurements. The earliest scan was recorded just at the beginning of the purging of the system, at a much too short time for significant removal of oxygen from the electrolyte to be attained. Indeed, the corresponding scan line registered by passing the tip over the holiday after 1 minute purging shows the oxidation of Fe(II) species at the UME, whereas the corresponding signal greatly diminished with the duration of the purging treatment, and could not be observed after 15 minutes, though the tip was scanned over the same place. That is, no Fe^{2+} ions are available for oxidation at the tip when the tip passes over the holiday, above the background signal. Thus, the removal of oxygen from the electrolytic phase results in no species being available to accept the electrons released in the oxidation of iron, and the corrosion process is thus hindered and eventually stopped. An additional observation from the inspection of Figure 1 can be made in relation to the asymmetry of the current signal measured at the tip when moving from left to right. This effect, and the corresponding background signals observed at all times, are related to convective effects due to the movement of the tip at the scan rate of 50 μm s^{-1}as it was shown previously [13].

An alternative procedure for oxygen removal from the electrolyte consisted is subjecting the electrolyte to a heating cycle up to 333 K under a nitrogen atmosphere, taking advantage of the decrease in solubility of oxygen in an aqueous solution with the increase of temperature [20]. But, only partial removal of oxygen from the solution is achieved in this way. Yet, the depletion of oxygen is sufficient to produce a reduction in the rate at which the exposed metal in the holiday corrodes. This effect is shown in Figure 2 by comparing the behaviour of the system for the naturally-aerated solution and for the solution after the heating cycle described above.

3.2. Monitoring of hydrogen peroxide soluble species in the proximity of the holiday during immersion in 0.1 M KCl when oxygen is removed from the electrolyte

Figure 3 shows the scan lines measured when the potential of the tip was set at +0.25 V vs. Ag/AgCl/KCl(sat.) before and after purging the test solution with nitrogen gas as described in the previous Section. In this case, the redox process monitored at the UME corresponds to the oxidation of hydrogen peroxide given by the equation:

$$H_2O_2 + 2\ OH^- \rightarrow 2e^- + O_2 + 2H_2O \qquad E^0 = 0.142 \text{ V vs. Ag/AgCl/KCl(sat.)} \quad (2)$$

The formation of hydrogen peroxide is a product formed during the reduction of oxygen at the cathodic sites occurring inside the holiday according to reaction:

$$O_2 + 2H_2O + 2\ e^- \rightarrow H_2O_2 + 2OH^- \quad (3)$$

Inspection of Figure 3 leads to the observation that the removal of soluble oxygen from the electrolyte leads to the measurement of smaller faradaic currents at the tip, closely matching the behaviour

previously observed for the oxidation of Fe(II) species. Then, the smaller availability of oxygen in the electrolytic phase for reaction (3) results in smaller amounts of hydrogen peroxide being formed in the cathodic half reaction. This is consistent with less iron soluble species being released from the metal too.

3.3. Monitoring of soluble oxygen in the proximity of the holiday during immersion in 0.1 M KCl when oxygen is removed from the electrolyte

The distribution of soluble oxygen in the proximity of the holiday during immersion in the test electrolyte could be monitored by setting the tip potential at -0.70 V vs. Ag/AgCl/KCl(sat.). The scan lines registered in the solution before and after bubbling nitrogen for 18 minutes are plotted in Figure 4. The curve measured in the naturally aerated solution shows rather high faradaic currents outside the holiday, which are consistent with the greater availability of oxygen in the electrolyte compared to the local concentrations of Fe^{2+} ions and hydrogen peroxide which originated exclusively from the corrosion reactions inside the holiday. When the tip is moved over the holiday, significantly smaller currents are measured at the tip, which are a clear indication that oxygen is consumed from the electrolyte during the corrosion reaction inside the defect. Purging of the solution with nitrogen results in a decrease of the faradaic currents measured at the tip when located both over the intact coating outside the holiday or over it. When sufficiently longer times are provided, namely 18 min, no significant differences are observed for the faradaic currents measured both inside and outside the holiday. This result closely matches the corresponding scan line for the oxidation of Fe(II) species at the tip shown in Figure 1 for the longest bubbling with nitrogen. Though complete removal of oxygen has not been attained yet, the decrease of oxygen availability is such that the corrosion process is effectively hindered inside the holiday.

The smaller effect towards oxygen renoval when the sample is heated under nitrogen atmosphere is better observed from the observation of figure 5. In this case, the currents measured at the tip after the treatment are smaller than those recorded in the naturally aerated solution, both inside and outside the holiday, though the oxygen consumption through the cathodic process is now smaller than in the aerated solution. This effect also matches the observations made above in the case of the oxidation of iron ionic species as deduced from the inspection of Figure 2.

A further comparison of the current signals observed by setting the tip potential to different applied values leads to the observation that the currents for the oxidation of hydrogen peroxide are ca. 50 times smaller than those related to the oxidation of Fe(II) species (cf. Figures 1 and 3). This is an indication that hydrogen peroxide is not the main reduction product for oxygen reduction according to reaction:

$$O_2 + 2H_2O + 4e^- \leftrightarrow 4OH^- \qquad (4)$$

This observation agrees well with the observation that the greatest local variation in concentration is experienced during the electroreduction of oxygen, as result of this molecule reacting on both the uncoated

metal at the defect and at the UME, thus originating a redox competition effect between both metallic substrates.

4. Conclusions

Major changes are observed in the faradaic currents measured at the SECM tip as result of oxygen removal from the electrolytic solution during the monitoring of oxygen, hydrogen peroxide and dissolved Fe(II) species.

The dissolution of iron and subsequent release of ionic iron species to the electrolyte is hindered as oxygen is progressively removed from the solution, which supports that the smaller availability of oxygen at the cathodic sites has a major effect on the corrosion rate of the metal inside the holiday.

Analogously, the decrease of oxygen availability to the reacting sites in the defective coating also results in less hydrogen peroxide being formed inside the holiday.

Acknowledgements:

This work was supported by the Ministerio de Ciencia y Tecnología (Madrid, Spain) and the European Regional Development Fund (Brussels, Belgium) under Project No. CTQ2009-14322. A grant awarded to JJS by the Gobierno de Canarias (Spain) to conduct a research stay at the University of La Laguna is gratefully acknowledged. Thanks are due to Sigma Coatings (Amsterdam, The Netherlands) for providing the coatings.

References:

1. A.C. Bastos, A.M. Simões, S. González, Y. González-García, R.M. Souto, Application of the scanning electrochemical microscope to the examination of organic coatings on metallic substrates, Prog. Org. Coat. 53 (2005) 177-182.
2. S.E. Pust, W. Maier, G. Wittstock, Investigation of localized catalytic and electrocatalytic processes and corrosion reactions with scanning electrochemical microscopy (SECM), Z. Phys. Chem. 222 (2008) 1463–1517.
3. L. Niu, Y. Yin, W. Guo, M. Lu, R. Qin, S. Chen, Application of scanning electrochemical microscope in the study of corrosion of metals, J. Mater. Sci. 44 (2009) 4511–4521.
4. Y. González-García, J.J. Santana, J. González-Guzmán, J. Izquierdo, S. González, R.M. Souto. Scanning electrochemical microscopy for the investigation of localized degradation processes in coated metals, Prog. Org. Coat. 69 (2010) 110-117.
5. R.M. Souto, Y. González-García, S. González, G.T. Burstein, Damage to paint coatings caused by electrolyte immersion as observed in situ by scanning electrochemical microscopy, Corros. Sci. 46 (2004) 2621-2628.

6. R.M. Souto, Y. González-García, S. González, Evaluation of the corrosion performance of coil-coated steel sheet as studied by scanning electrochemical microscopy, Corros. Sci. 50 (2008) 1637-1643.
7. R.M. Souto, Y. González-García, S. González, Characterization of coating systems by scanning electrochemical microscopy: surface topology and blistering, Prog. Org. Coat. 65 (2009) 435–439.
8. E. Salamifar, M.A. Mehrgardi, M.F. Mousavi, Ion transport and degradation studies of a polyaniline-modified electrode using SECM, Electrochim. Acta 54 (2009) 4638–4646.
9. R.M. Souto, Y. González-García, S. González, G.T. Burstein, Imaging the origins of coating degradation and blistering caused by electrolyte immersion assisted by SECM, Electroanalysis 21 (2009) 2569-2574.
10. J. Kwak, A.J. Bard, Scanning electrochemical microscopy. Theory of the feedback mode, Anal. Chem. 61 (1989) 1221-1227.
11. R.M. Souto, Y. González-García, J. Izquierdo, S. González, Examination of organic coatings on metallic substrates by scanning electrochemical microscopy in feedback mode: revealing the early stages of coating breakdown in corrosive environments, Corros. Sci. 52 (2010) 748-753.
12. C. Bragato, S. Daniele, M.A. Baldo, G. Denuault, Oxygen as redox mediator in scanning electrochemical microscopy. Application to the study of localised acid attack of marble, Annali di Chimica 92 (2002) 153–161.
13. R.M. Souto, Y. González-García, S. González, *In situ* monitoring of electroactive species by using the scanning electrochemical microscope. Application to the investigation of degradation processes at defective coated metals, Corros. Sci. 47 (2005) 3312-3323.
14. A. Simões, D. Battocchi, D. Tallman, G. Bierwagen, Assessment of the corrosion protection of aluminium substrates by a Mg-rich primer: EIS, SVET and SECM study, Prog. Org. Coat. 63 (2008) 260–266.
15. R.M. Souto, L. Fernández-Mérida, S. González, SECM imaging of interfacial processes in defective organic coatings applied on metallic substrates using oxygen as redox mediator, Electroanalysis 21 (2009) 2640-2646.
16. J.J. Santana, J. González-Guzmán, L. Fernández-Mérida, S. González, R.M. Souto, Visualization of local degradation processes in coated metals by means of scanning electrochemical microscopy in the redox competition mode, Electrochim. Acta 55 (2010) 4488-4494.
17. Y. González-García, G.T. Burstein, S. González, R.M. Souto, Imaging metastable pits on austenitic stainless steel in situ at the open-circuit corrosion potential, Electrochem. Commun. 6 (2004) 637-642.
18. A.C. Bastos, A.M. Simões, S. González, Y. González-García, R.M. Souto, Imaging concentration profiles of redox-active species in open-circuit corrosion processes with the scanning electrochemical microscope, Electrochem. Commun. 6 (2004) 1212-1215.
19. Y. González-García, S. González, R.M. Souto, Electrochemical and structural properties of a polyurethane coating on steel substrates for corrosion protection, Corros. Sci. 49 (2007) 3514-3526.
20. D. Tromans, Temperature and pressure dependent solubility of oxygen in water: a thermodynamic analysis, Hydrometallurgy 48 (1998) 327-342.

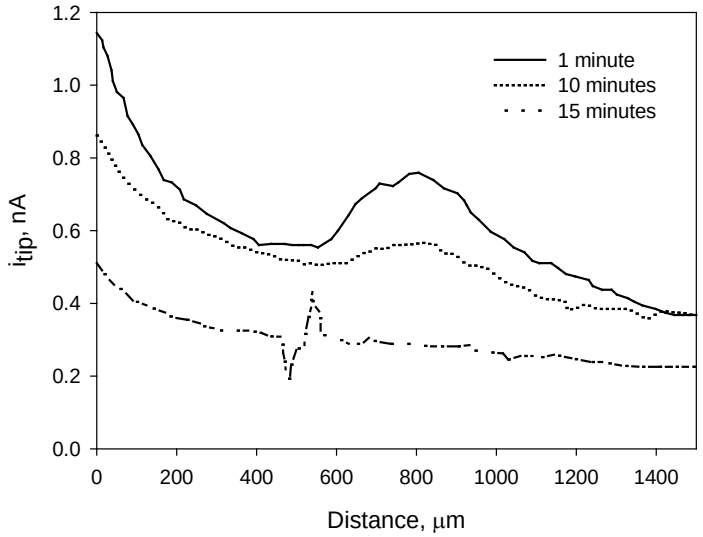

Figure 1 - Scans lines each representing a single scan of the probe trip across the holiday in the organic coating after immersion in 0.1 M KCl aqueous solution while nitrogen is purged through the electrolyte for the durations indicated in the figure. The tip potential was +0.60 V vs. Ag/AgCl/KCl(sat.). Tip-substrate distance: 10 μm; scan rate: 50 μm s^{-1}.

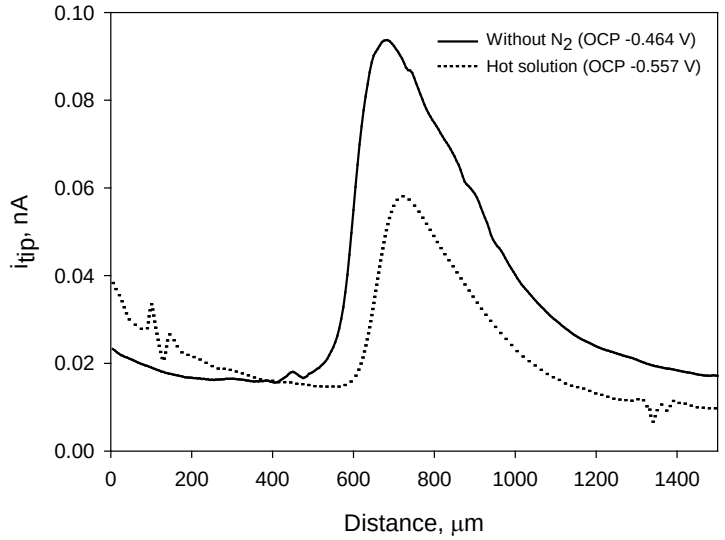

Figure 2 - Scans lines each representing a single scan of the probe trip across the holiday in the organic coating after immersion in 0.1 M KCl aqueous solution just before and after producing a heating cycle in the electrolyte up to 333 K. The tip potential was +0.60 V vs. Ag/AgCl/KCl(sat.). Tip-substrate distance: 10 μm; scan rate: 50 μm s^{-1}.

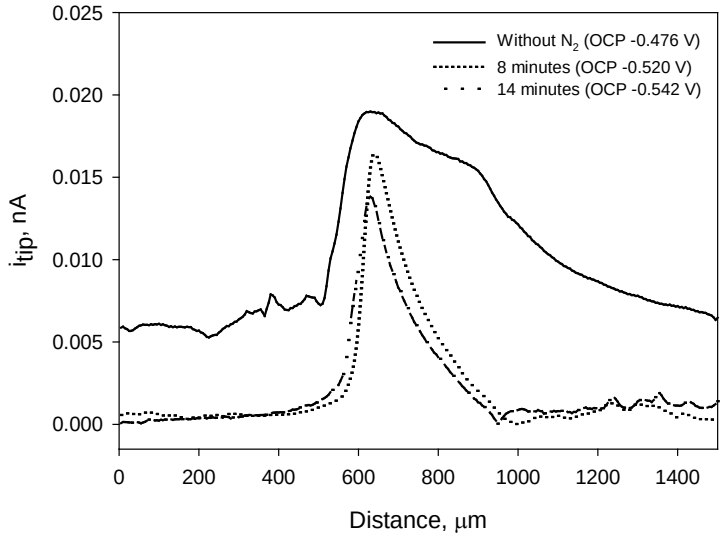

Figure 3 - Scans lines each representing a single scan of the probe trip across the holiday in the organic coating after immersion in 0.1 M KCl aqueous solution while nitrogen is purged through the electrolyte for the durations indicated in the figure. The tip potential was +0.25 V vs. Ag/AgCl/KCl(sat.). Tip-substrate distance: 10 μm; scan rate: 50 μm s^{-1}.

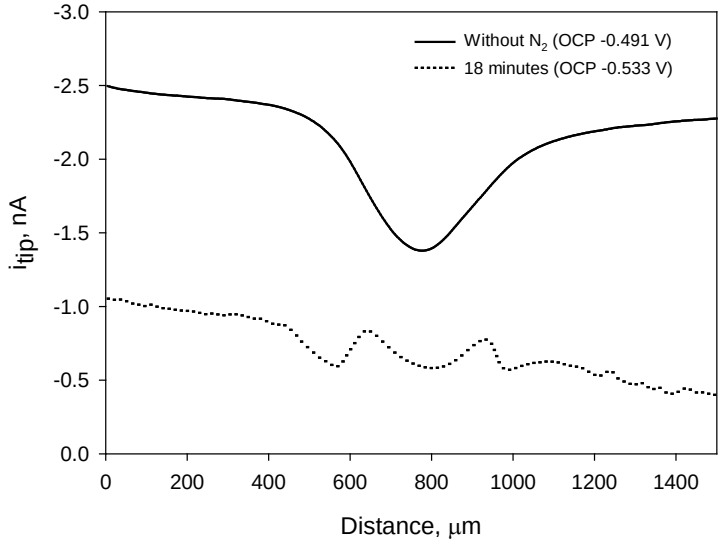

Figure 4 - Scans lines each representing a single scan of the probe trip across the holiday in the organic coating after immersion in 0.1 M KCl aqueous solution while nitrogen is purged through the electrolyte for the durations indicated in the figure. The tip potential was -0.70 V vs. Ag/AgCl/KCl(sat.). Tip-substrate distance: 10 μm; scan rate: 50 μm s^{-1}.

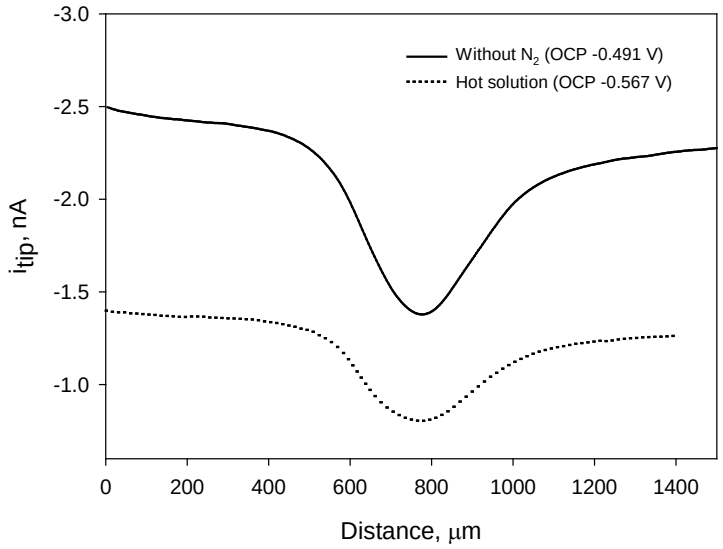

Figure 5 - Scans lines each representing a single scan of the probe trip across the holiday in the organic coating after immersion in 0.1 M KCl aqueous solution just before and after producing a heating cycle in the electrolyte up to 333 K. The tip potential was -0.70 V vs. Ag/AgCl/KCl(sat.). Tip-substrate distance: 10 μm; scan rate: 50 μm s^{-1}.